  Bull. Chem. Soc. Jpn., 60, 49—54 (1987)

Time-Resolved Unimolecular Reactions of Pyridine Ions by Means of Trapped-Ion Mass Spectrometry

Ryuichi ARAKAWA* and Yozaburo YOSHIKAWA
Institute of Chemistry, College of General Education, Osaka University,
Toyonaka, Osaka 560
(Received June 16, 1986)

The electron-impact ionization-efficiency curves for the $C_5H_5N^{+\cdot} \rightarrow C_4H_4^{+\cdot} + HCN$ dissociation have been measured as a function of the ion-source-residence time by means of trapped-ion mass spectrometry (TIMS). The ionization-efficiency curves for residence times of 5 and 700 μs were fitted by QET calculation, assuming dissociation-rate models. A kinetic shift of 0.3 eV was observed from the time-dependent appearance energy measurements. The fragmentation of metastable ions was first sampled for the ion-source residence time of 0—100 μs. The preferable rate model was determined by the analysis of the ionization-efficiency curves and the metastable ion fragmentations. Time-resolved kinetic energy releases for pyridine and perdeuteriopyridine have been explained in terms of excess energy drop of metastable ions with their lifetime.

The $C_4H_4^+$ ion is one of the major fragments from benzene and pyridine in their mass spectra. The appearance energy of the pyridine reaction (Eq. 1) has been measured by a wide variety of experimental techniques.[1-5]

$$C_5H_5N^{+\cdot} \longrightarrow C_4H_4^{+\cdot} + HCN. \quad (1)$$

One of the main problems in these measurements is the so-called "kinetic shift," the excess energy required to produce a detectable dissociation of a polyatomic ion. Ion-trapping techniques are favored for clarifying this kind of problem. There have been two reports of experimental results for the dissociation of trapped pyridine ions. One was the study of Rosenstock et al.[6] by means of photoion-photoelectron coincidence (PIPECO) mass spectrometry, with a variable ion-source-residence time. The dissociation threshold energy at 0 K was determined by their detailed analysis of time-dependent breakdown curves obtained from the first derivative of photoionization curves with a microsecond ion-residence time. The other was studied by Lifshitz[7] using trapped ion mass spectrometry, with a millisecond ion-storage time. The second derivative of electron-impact ionization curves produced the breakdown curves.

In these two studies, a shift observed for time-resolved breakdown curves was used for evaluating the kinetic shift. The measurements of the breakdown curve shift give us less erroneous information about the kinetic shift than conventional appearance energy measurements for metastable ions, e. g., a semilog plot. This is because metastable ions usually have quite a low intensity relative to the normal ion intensity. Compared with the PIPECO experiment, the TIMS experiment can easily change the ion-residence time from zero to several milliseconds, so that unimolecular reactions of rate constants ranging from 10^2 to 10^5 s^{-1} can be observed. However, its energy definition for ionized precursors is rather uncertain because of electron-impact ionization.

Recently, the fragmentation of the bromobenzene ion to the phenyl cation has been studied by Lifshitz and her co-workers[8] using time-resolved photoionization mass spectrometry (TPIMS). Photoionization efficiency (PIE) curves at ion-residence times of 2 m s and 6 μs have been, for the first time, measured and compared with the calculated PIE curves near the threshold energy. A critical appearance energy was determined from the calculation of the quasi-equilibrium theory(QET). The TPIMS technique has employed a cylindrical ion-trap chamber to store ions over milliseconds, because the variable-time PIPECO technique limits ion-source-residence time to a microsecond time scale.

In the present work, electron-impact ionization efficiency (EIE) curves for the pyridine reaction (Eq. 1) have been measured as a function of the ion-source-residence time. Then, we observed a shift of time-resolved daughter EIE curves near the threshold energy, although the electron-impact energy had an spread of ≈1 eV. The EIE curves moved to a lower energy side with an increase in the ion-residence time. The time-resolved EIE curves will be analyzed by QET calculation using two available unimolecular rate models. The EIE curve can be expressed in the mathematical form of double integrations of breakdown curves, while the PIE calculation involves a single integration of breakdown curves with respect to energy. A difficulty in the EIE curve calculation is to estimate the internal energy distribution of parent ions ionized with a variable incident electron energy. Here, we estimated the internal energy distribution on the basis of the threshold behavior of the electron ionization. In addition, the energy spread of incident electrons should be convoluted for the EIE calculation.

The metastable peak intensity and the kinetic energy release have not been measured for a wide range of ion-source-residence times. Two rate models for the pyridine reaction (Eq. 1) have been reported using the PIPECO technique.[3,6] We will discuss the

validity of these rate models by analyzing the time-resolved metastable ion fragmentation, because its fragmentation depends greatly on the unimolecular rate constant. Moreover, the time-resolved kinetic-energy-release measurement can closely test an empirical relation between the kinetic energy release and the internal excess energy of precursor ions.

Experimental

The ion trapping technique employed has been described in detail by Herod and Harrison[9] and by Lifshitz.[10] Ions were produced when a negative pulse was applied to a Rhenium filament. A continuous 5-eV electron beam, forming a negative potential well, was used to trap the ions. The well-depth should be greater than the thermal kinetic energy of the trapped ions.[11] A small negative bias on a repeller plate is also necessary for effective trapping. At a known delay time after the ionizing pulse, a positive pulse, 6 μs in duration and 6 eV in height, was applied to a repeller electrode to remove ions for mass analysis. The ion-trapping efficiency was examined by the use of Kr or pyridine ions. These ions were stored up to several milliseconds without any serious decrease in the trapped-ion concentration. An ionizing pulse 2 μs in duration was applied to the filament at 1-ms intervals. The nominal electron energy was varied by changing the pulse height applied to the filament.

A home-built tandem mass spectrometer[12] was used to measure the fragment-ion abundance and the kinetic-energy release in the metastable ion dissociation. Fragment ions produced by unimolecular decomposition occurring in the second-field free region between two magnets were detected by means of a pulse-counting method. Their intensities were then analyzed by means of a microcomputer. The temperature of the ion source was 423 K. The ion-accelerating voltage was 1.5 kV. The ion-source pressure was kept at 2×10^{-6} Torr (1 Torr=133.32 Pa). The collisional induced reaction were negligible, because the pressure in the field-free region was always less than 1×10^{-6} Torr. The samples of pyridine and perdeuteriopyridine (99% atom D; MERCK) were commercially obtained.

Results and Discussion

Time-Resolved EIE Curves and Appearance Energies. Figure 1 displays the EIE curves of daughter-($C_4H_4^+$) and parent($C_5H_5N^+$) ions for the delay times of 5 and 700 μs. The EIE data have been accumulated for several hours because of low counting rates near the reaction onset. A kinetic shift of about 0.3 eV was observed near the onset. In the previous TIMS experiment,[7] the normalized second derivatives of the experimental EIE curves yielded the breakdown curves. A crossing point of daughter and parent fractions in the breakdown curve moved with the delay time, and its shift was compared with that of the QET calculation. The breakdown curves have a width of a few eV at the nominal electron energy. Thus, it should be emphasized that time-resolved EIE curves, as well as the PIE curves in the TPIMS analysis, should be analyzed in a narrow energy range above the onset.

The time-resolved EIE of the daughter ion at a nominal electron energy, V, can be written in this form:

$$\mathrm{EIE}(V,t) = c\int_0^\infty m(E_t-V) \times\left[\int_{AE_o}^{E_t} f(E_t,E)(1-\exp(-k(E)t))dE\right]dE_t. \quad (2)$$

Here, c is the constant; t is the ion residence time; $m(E_t-V)$ is the instrumental-electron energy distribution; E_t is the total electron energy, defined as V plus the energy of the electron emitted from the filament; $f(E_t,E)$ is the internal energy distribution at the electron-impact energy, E_t; E is the internal energy of the parent ion; $k(E)$ is the unimolecular rate constant, and AE_o is the appearance energy at 0 K.

Morrison has proposed that the EIE second derivatives for inert gases yield the electron-energy distribution, reversed with respect to the energy scale.[13] In the present case, the $m(E_t-V)$ distribution was obtained by differentiating the experimental helium EIE. The half-width of $m(E_t-V)$ was found to be 0.8 eV. From the threshold law of ionization,[14] the internal energy distribution is given by $f(E_t,E)=p(E)\cdot(E_t-E)^{K-1}$, where $p(E)$ is the energy deposition function; the exponent K gives the number of electrons that leave the collision complex; $K=1$ for

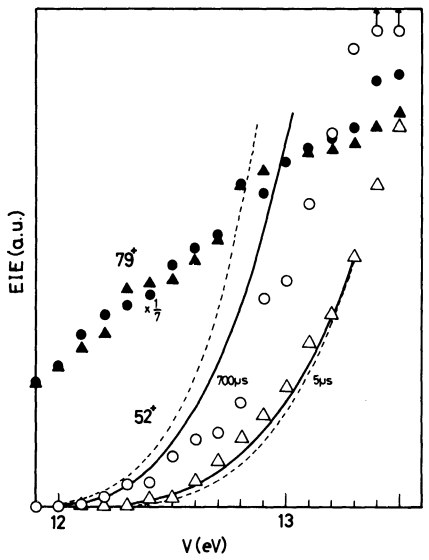

Fig. 1. Time-resolved electron ionization efficiency (EIE) curves measured with a 0.1 eV step of the nominal electron energy V. Experimental EIEs plotted on an arbitrary unit: ○, △, $C_4H_4^+$ fragment (52^+) for the delay times of t=700 and 5 μs, respectively; ●, ▲, parent ion (79^+). The EIE calculations based on the two available $k(E)$ models: ——, Eland et al.[3]; ----, Rosenstock et al.[6]. The calculated EIE curves were normalized at V=13.3 eV for the 5 μs curve.

photon impact, and $K=2$ for electron impact. The first derivative of the total PIE reported by Goffart et al.[15] was assumed to represent the $p(E)$ function upon ionization by electron impact. The mean vibrational energy of the pyridine molecules was 0.13 eV at 423 K. This thermal distribution was not considered in the EIE calculation, because the thermal effect was much less than the broad $m(E_t-V)$ distribution.

The experimental EIE curves were fitted using the two rate models proposed by Eland et al.,[3] $k_E(E)$, and by Rosenstock et al.,[6] $k_R(E)$. The $k_E(E)$ model has a tight transition state to fit their experimental $k(E)$ with the threshold energy of $AE_O=11.8$ eV. $k_R(E)$ is a loose model having $AE_O=12.15$ eV, which fits the measured crossover shift and the crossover energy of the breakdown curves. As a result, $k_R(E)$ has a somewhat steeper energy dependence than does $k_E(E)$.

The short delay time of 5 μs corresponds to the actual reaction time of 8 μs in the ion source. Figure 1 indicates that agreement with the experimental EIE curves is better for the $k_E(E)$ model than for the $k_R(E)$ model. This is consistent with the breakdown curve results[7] for fitting the experimental crossover shift for delay times of 5 and 1000 μs. From the time-resolved EIE calculation, the shift near the onset proved to depend only on the magnitude of $k(E)$ and to increase as the rate decreased. These results were actually due to the term of $1-\exp(-k(E)t)$ in Eq. 2. The $k_R(E)$ rate model, therefore, yielded a larger EIE shift than the $k_E(E)$ model, as is shown in Fig. 1; the rate constant near the threshold is smaller for $k_R(E)$ than for $k_E(E)$, because the $k_R(E)$ model has a higher reaction threshold. Thus, the amount of EIE shift is principally affected by the AE_O value.

The appearance energies, AE, of the $C_4X_4^+$ (X=H,D) ion, measured as a function of the delay time for pyridine and deuteriopyridine, are shown in Fig. 2. The convenient procedure for AE determination has been described by Burgers and Holmes[16] and by Gefen and Lifshitz.[17] On the basis of this procedure, we obtained the experimental AE value at a known delay time by comparing the EIE intensity of the fragment with that of a reference over a narrow range of ionizing-electron energies. The EIE comparison is usually made at the energy of ≈2 eV, far from the real onset, where the EIE intensity is statistically sufficient. The EIE curve for pyridine ions was employed as a reference. The ionization energy of pyridine (9.36 eV) was obtained by calibration with the ionization energies of benzene (9.24 eV)[18] and methyl acetate (10.27 eV).[2]

Lifshitz[7] has calculated the dependence of the delay time on the appearance energies using an equation for a minimum detectable ion signal developed by Gordon and Reid.[19] We recalculated the AE curve with the $k_E(E)$ rate model, as is shown in Fig. 2. The experimental AE of the $C_4H_4^+$ ion levels off at $AE=12.1\pm0.1$ eV. The kinetic shift of 0.3 eV for the $C_4H_4^+$ fragment was obtained from the AE gap between short and long reaction times. This AE gap agreed with the calculated one. In the present AE measurement, the EIE comparison was made at around $V=14$ eV. On the other hand, the time-resolved EIE measurement due to data accumulation produced an EIE shift of ≈0.3 eV at the lower energy of $V=12.5$ eV, as is shown in Fig. 1. Hence, it is worth

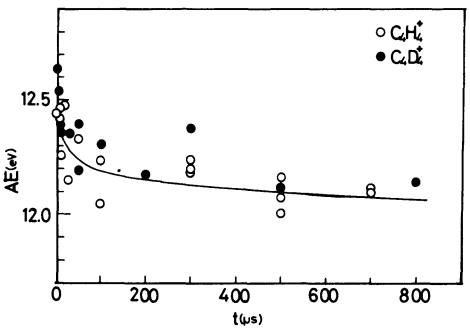

Fig. 2. Time dependent appearance energies AE for the reaction $C_5X_5N^{+\cdot}\rightarrow C_4X_4^{+\cdot}+XCN$(X=H, D). Experimental AEs at the ion source temperature of 423 K are indicated by open circles (X=H) and filled (X=D). The smooth line is the calculated AE for $C_4H_4^+$ using the rate model of Eland et al. Procedure for time-dependent AE calculation has in detail been described in Ref. 17. The minimum daughter concentration was calculated by setting $AE=12.5$ eV for $t=0$ μs. Since the detection sensitivity was independent of the delay time, AE for given delay time was then determined so as to produce the same concentration as calculated for $t=0$ μs.

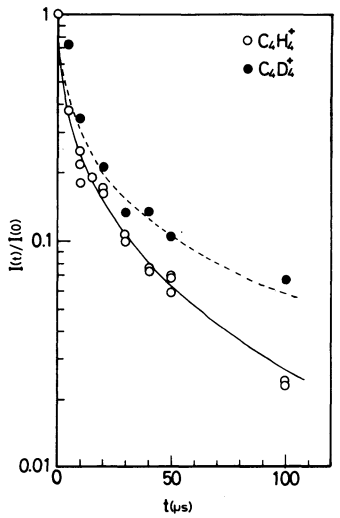

Fig. 3. The metastable ion abundances $I(t)$ for $C_4H_4^+$ (○) and $C_4D_4^+$(●) measured as a function of delay times when $V=20$ eV. The data are nomalized at $t=0$ μs. The solid and dashed curves are the calculated $I(t)$ for $C_4H_4^+$ using the rate models of $k_E(E)$ and $k_R(E)$, respectively.

noting that the EIE shift measured is rather independent of the detection sensitivity of EIE. Finally, the rate model of Eland et al. is the preferable model for fitting the time-resolved EIE and AE curves. The AE values for the $C_4D_4^+$ fragment, as a whole, have a tendency to exceed those for the $C_4H_4^+$ fragment. The AE_0 value for perdeuteriopyridine was estimated by applying a zero-point vibrational energy correction[5]; at most, it proved 0.1 eV greater than that for pyridine.

Fragmentation of Metastable Ions. The relative abundance of the $C_4X_4^+$ resulting from the metastable transition of $C_5X_5N^+$ (X=H,D) was measured in the range of t=0—100 μs, as is shown in Fig. 3. For example, the $C_4H_4^+$ fraction relative to the parent ion was 3.1×10^{-2} at t=0 μs. The fragment abundance, $I(t)$, is given[20] by:

$$I(t) = c\int_0^\infty m(E_t-V) \times\left[\int_{AE_0}^{E_t} f(E_t-E)w(E)(k(E)/k_t(E))dE\right]dE_t, \quad (3)$$

where $k_t(E)=k(E)+k_n(E)$ is the total decay rate, $k_n(E)$ is a nondissociative rate such as the infrared radiative decay and the collisional relaxation in the ion source, and $w(E)=\exp(-k_t(E)t_1)-\exp(-k_t(E)t_2)$ is a fraction of the metastable-ion dissociation. (t_2-t_1) is the time ions spend in the second field-free region, where metastable ions are produced; $t_1=6.8+t$ and $t_2=11.8+t$ μs. The $I(t)$ curves for the $C_4H_4^+$ fragment were calculated with two $k(E)$ models in the case of $k_n(E)=0$. The calculated curve for the $k_E(E)$ model is in good agreement with the experimental curve, as is shown in Fig. 3. In this manner, the measurements of the time-resolved metastable peak abundances enable us to determine the $k(E)$ model, because the $I(t)$ curve is dependent on a rising steepness of $k(E)$. The rates corresponding to a peak of the $w(E)$ function when t=0 and 100 μs are $k(E)=1.1\times10^5$ and 9.1×10^3 s^{-1} respectively. These rates mainly contribute to the metastable fragmentation.

The approximate collisional relaxation rate is given by the Langevin ion-molecule reaction theory.[21] The relaxation rate of a bimolecular reaction is 80 s^{-1} at the present sample density if the polarizability of benzene, 10.3×10^{-24} cm^3, is taken as that of pyridine. Dunbar[22] has suggested that an upper limit on the lifetime of metastable-ion decomposition is determined by the competing relaxation of the infrared radiative cooling. This upper limit lies in the range of 15—60 s^{-1} for polyatomic molecules. The effects of the radiative decay on time-resolved PIE curves have been discussed in the case of a bromobenzene reaction.[8]

The nondissociative rate, $k_n(E)$, is, at most, 150 s^{-1}, as has been estimated above. This amount of $k_n(E)$ proved to have no effect on the quantity of metastable-ion fragmentation. For $k(E)\leq10^3$ s^{-1}, small values of $k_t(E)t_1$ and $k_t(E)t_2$ lead to $w(E)k(E)/k_t(E)\simeq(t_2-t_1)k(E)$ in Eq. 3. For $k(E)>10^3$ s^{-1}, $k_n(E)$ is negligible compared with $k(E)$. Thus, $I(t)$ is independent of $k_n(E)$.

Figure 4 represents the fragmentations of the metastable $C_4X_4^+$ ion by the loss of a hydrogen atom and a hydrogen molecule. The relative intensity of the two channels is nearly equal throughout the delay time.

Time-Resolved Kinetic Energy Release (KER). A metastable peak shape and its width are a very sensitive measure of the KER in unimolecular reactions.[23] In principle, a reaction with a large kinetic shift should show a large change in the KER with a increase in the metastable-ion lifetime. This has been demonstrated by Gefen and Lifshitz[17] in the case of iodobenzene. The KER value T, as determined by the peak analysis,[24] is given by:

$$T = m_1^2HV/(16m_2^3m_3)d^2 \quad (4)$$

Here, m_1 is the mass of the parent ion; m_2 and m_3 are the mass of the fragment ion and the neutral respectively; HV is the ion-accelerating voltage, and d is the peak width of the metastable ion, corrected by the normal peak width in units of the atomic mass. The experimental KER values at a half maximum, $T_{1/2}$, are listed in Tables 1 and 2. The error limits represent the standard deviation of several runs.

A simple method for the evaluation of the average KER $\langle T\rangle$ for a Gaussian-type metastable peak was described by Holmes and Osborne.[25] The $\langle T\rangle$ values were obtained from their relationship between the $\langle T\rangle/T_{1/2}$ ratio and the peak shape parameter n(=1.8 for the present case), which had itself been derived from width ratios at the given peak heights. Accord-

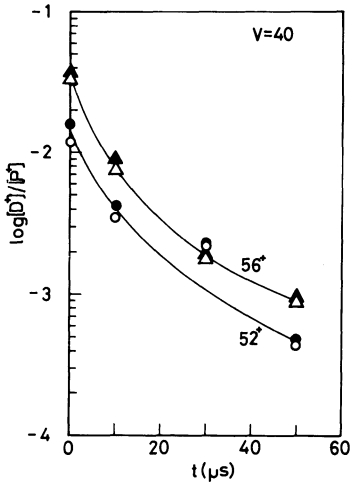

Fig. 4. Time-resolved abundances produced by two parallel fragmentations by X and X_2 loss from $C_4H_4^+$ (X=H, D) precursors. Symbols represent fragments by the H(○), H_2 (●), D (△), and D_2 (▲) loss. The abundances relative to the parent, $[D^+]/[P^+]$ at V= 40 eV are plotted on a logarithmic scale. The lines are for easy comparison.

Table 1. Time-Resolved Kinetic Energy Releases $T_{1/2}$ for the Pyridine Metastable Transition of $C_5X_5N^{+\cdot} \longrightarrow C_4X_4^{+\cdot} + XCN(X=H, D)$

$t/\mu s$	X=H			X=D		
	$T_{1/2}$/meV	E^*/eV[a]	E_p/eV[b]	$T_{1/2}$/meV	E^*/eV	E_p/eV[c]
0	49±10	1.5±0.3	0.90	53	1.6	1.2
5	41±8	1.3±0.3				
10	29	0.9	0.80	43	1.3	1.0
20	23	0.7				
30	29	0.9	0.70	36	1.1	0.90
40	8	0.3				
50	8	0.3	0.65	33	1.0	0.85
100	0		0.60	35	1.0	0.80

a) E^* represents the excess energy of metastable ions above the reaction threshold, which was obtained from the experimental $T_{1/2}$ values according to the relation of Haney and Franklin.[26] b) E_p is the peak energy for the $w(E)$ function above the threshold. It corresponds to the $k(E_p)=\ln(t_2/t_1)/(t_2-t_1)$ rate, where t_1 and t_2 are respectively, the entrance and the exit time in the second field-free region. The $k(E)$ model of Eland et al. was used for this calculation. c) The unimolecular rate constant for deuteriopyridine was obtained by directly computing the harmonic oscillator eigenstate sums and densities. The vibrational frequencies used were given in Ref. 5.

Table 2. Time-Resolved Kinetic Energy Releases $T_{1/2}$ for $C_4X_3^+$ and $C_4X_2^+$ Fragments from Metastable $C_4X_4^+$(X=H, D) Ions

$t/\mu s$	$T_{1/2}$/meV			
	$-H$[a]	$-H_2$	$-D$	$-D_2$
0	90±15	330±50	180	400
10	0	160	180	330
20	0	220	—	—
30	0	100	140	200
50	—	—	100	200

a) The notation of $-H$ represents the hydrogen atom loss.

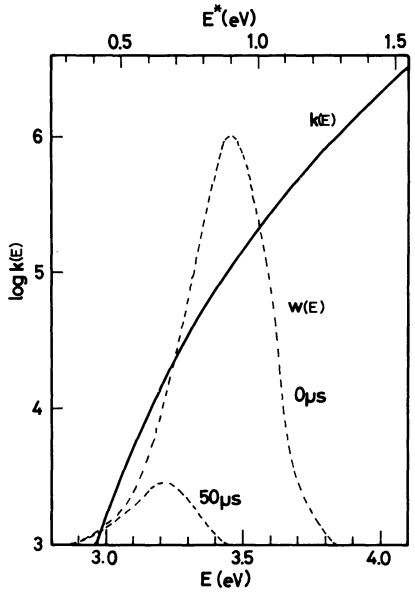

Fig. 5. The relationship of $k(E)$ and $w(E)$ for the pyridine reaction. $k(E)$ indicates the unimolecular rate constant of Eland et al. The $w(E)$ functions, as defined in Eq. 3, for delay times of $t=0$ and 50 μs are linearly plotted on an arbitrary unit vs. the internal energy E above ionization threshold. E^*(upper scale) represents the excess energy above reaction threshold.

ing to the empirical formula of Haney and Franklin,[26] $\langle T\rangle=E^*/(0.44N)$, the average KER $\langle T\rangle$ is related to the excess energy(E^*) of metastable ions above the threshold. Here, N is the number of vibrational degrees of freedom of the parent ion. $\langle T\rangle$ should approach zero as E^* approaches zero if there is no reverse activation energy. The excess energies estimated from the experimental $T_{1/2}$ values are given in Table 1.

Generally, the KER value decreases with the lifetime of metastable ions. The fragmentation takes place only for metastable ions with a limited range of excess energy, as defined by the $w(E)$ function in Eq. 3. The $w(E)$ curves for $t=0$ and 50 μs were calculated with the $k_E(E)$ model, as shown in Fig. 5. The increase in the delay time lowers the peak position of the $w(E)$ curve. A peak energy E_P of $w(E)$ above the threshold can be representative of the average internal energy, compared with E^*. The E^* values for every delay time in Table 1 are estimated to have the error limit of ≈0.3 eV. The experimental E^* values are roughly reproduced by the calculated E_P values, except at $t=0$ μs. The reaction of deuteriopyridine has slower rate constants than that of pyridine. This causes the larger KERs for deuteriopyridine than for pyridine; The excess energy of decomposing ions declines consistently with the increase in the rate constant. Strictly speaking, the metastable peak should be analyzed by taking the internal energy distribution into account. An sttempt to determine time-resolved KERs for pyridine has been made in a previous TIMS

study.[7] A rough estimate of the maximum KER ratio at delay times of 0 and 100 μs was $T_{max}(0\ \mu s)/T_{max}(100\ \mu s)=3.5$. The maximum KER, which reflects the internal excess energy, was obtained from the widths at the base of the peaks above the noise level. This KER ratio is far beyond the calculated E_P ratio of 1.5 between $t=0$ and 100 μs.

Table 2 represents time-resolved KERs by the X and X_2 loss of the metastable $C_4X_4^+$ ion. Our KER values of $T_{1/2}=90$ and 330 meV for $C_4H_4^+$ at $t=0$ μs are comparable to those of $T_{1/2}=49$ and 399 mV[27] respectively. As in the pyridine reaction, the $C_4D_4^+$ reaction always has a greater KER than the $C_4H_4^+$.

The present study has advanced understanding of the unimolecular decomposition of pyridine ions. The reaction rate model of Eland et al. proved to be best for time-resolved measurements of both the EIE curve and the metastable peak. In particular, the analysis of the EIE shift near onset permitted a determination of the AE_0 threshold energy, whereas the measurement of the metastable-ion fragmentation was effective for evaluating the rising steepness of $k(E)$. The empirical formula of Haney and Franklin was not ruled out by the present time-resolved KER measurements with the metastable-ion lifetime of 0—100 μs.

We wish to thank Professor C. Lifshitz, Department of Physical Chemistry, The Hebrew University of Jerusalem, for her helpful discussions and advice.

References

1) B-Ö. Jonssen, E. Lindehelm, and A. Skerbele, *Int. J. Mass Spectrom. Ion Phys.*, **3**, 385 (1969).
2) H. M. Rosenstock, K. Draxl, B. W. Steiner, and J. T. Herron, *J. Phys. Chem. Ref. Data*, **6**, Suppl. 1 (1977).
3) J. H. D. Eland, J. Berkowitz, H. Shulte, and R. Frey, *Int. J. Mass Spectrom. Ion Phys.*, **28**, 297 (1978).
4) H. M. Rosenstock and K. E. McCulloh, *Int. J. Mass Spectrom. Ion Phys.*, **25**, 327 (1977).
5) R. Arakawa, M. Arimura, and Y. Yoshikawa, *Int. J. Mass Spectrom. Ion Processes*, **64**, 227 (1985).
6) H. M. Rosenstock, R. Stockbauer, and A. Parr, *Int. J. Mass Spectrom. Ion Phys.*, **38**, 323 (1981).
7) C. Lifshitz, *J. Phys. Chem.*, **86**, 606 (1982).
8) Y. Malinovich, R. Arakawa, G. Haase, and C. Lifshitz, *J. Phys. Chem.*, **89**, 2253 (1985).
9) A. A. Herod and A. G. Harrison, *Int. J. Mass Spectrom. Ion Phys.*, **4**, 415 (1970).
10) C. Lifshitz, *Mass Spectrom. Rev.*, **1**, 309 (1982).
11) F. A. Baker and J. B. Hasted, *Philos. Trans. R. Soc. London*, **A261**, 33 (1966).
12) M. Arimura and Y. Yoshikawa *Mass Spectrom. (Jpn.)*, **30**, 183 (1982).
13) J. D. Morrison, *J. Chem. Phys.*, **21**, 1767 (1953).
14) M. R. H. Rudge, *Rev. Mod. Phys.*, **40**, 564 (1968); M. R. H. Rudge, and M. J. Seaton, *Proc. Phys. Soc.*, **83**, 183 (1982).
15) C. Goffart, J. Momigny, and P. Natalis, *Int. J. Mass Spectrom. Ion Phys.*, **3**, 371 (1969).
16) P. C. Burgers and J. L. Holmes, *Org. Mass Spectrom.*, **17**, 123 (1982).
17) S. Gefen and C. Lifshitz, *Int. J. Mass Spectrom Ion Phys.*, **58**, 251 (1984).
18) T. Baer, G. D. Willett, D. Smith, and J. S. Phillips, *J. Chem. Phys.*, **70**, 4076 (1979).
19) S. Gordon and N. W. Reid, *Int. J. Mass Spectrom. Ion Phys.*, **18**, 379 (1975).
20) A. N. H. Yeo and D. H. Williams, *J. Am. Chem. Soc.*, **93**, 395 (1971).
21) G. Gioumousis and D. P. Stevenson, *J. Chem. Phys.*, **29**, 294 (1958).
22) R. C. Dunbar, *Int. J. Mass Spectrom. Ion Phys.*, **54**, 109 (1983).
23) R. G. Cooks and J. H. Beynon, *J. Chem. Phys.*, **51**, 437 (1974).
24) S. T. Pratt and W. A. Chupka, *Chem. Phys.*, **62**, 153 (1981).
25) J. L. Holmes and A. D. Osborne, *Org. Mass Spectrom.*, **16**, 236 (1981); J. L. Holmes and J. K. Terlouw, *Org. Mass Spectrom.*, **15**, 383 (1980).
26) M. A. Haney and J. L. Franklin, *J. Chem. Phys.*, **48**, 4903 (1968); C. E. Klots, *J. Chem. Phys.*, **58**, 5364 (1973).
27) C. Lifshitz, D. Gibson, K. Levsen, and I. Dotan, *Int. J. Mass Spectrom. Ion Phys.*, **40**, 157 (1981).